Reactions ^{58}Ni(p,γ)^{59}Cu and ^{58}Ni(p,p$'\gamma$)^{58}Ni from 0.75 to 5.00 MeV

G. U. Din
Department of Physics, King Saud University, Riyadh, Saudi Arabia

J. A. Cameron, V. P. Janzen, and R. B. Schubank
Tandem Accelerator Laboratory, McMaster University, Hamilton, Ontario, Canada L8S 4K1
(Received 10 February 1984)

The system p+^{58}Ni has been investigated at laboratory energies from 0.75 to 5.00 MeV. Continuous yield curves in the (p,γ) and (p,p$'\gamma$) channels were obtained with a resolution of about 2 keV. In the capture channel, 190 resonances were identified. For 56 resonances, in regions of possible analog states, γ-ray spectra were measured. Spins of 28 of the stronger resonances were determined from γ-ray angular distributions. Spins of the weaker resonances were inferred from their decay branching. Eighteen analog state candidates were identified, allowing a systematic survey of isobaric analogs up to 3 MeV in the parent ^{59}Ni. Several of the analogs are fragmented, including the $g_{9/2}$ state at 3.550 MeV, for which a nearby companion at 3.480 MeV was found. A further $\frac{9}{2}^+$ resonance some 0.7 MeV below the analog state at 2.839 MeV was also found. In addition to the resonant state information, the γ decay spectra and angular distributions lead to the establishment of five new bound levels of ^{59}Cu, at 2.993, 3.574, 3.729, 3.930, and 4.465 MeV. Nine levels, previously observed only in particle transfer reactions, at 3.309, 3.551, 3.699, 4.072, 4.207, 4.307, 4.441, 4.530, and 4.917 MeV, were seen. The decay schemes of these and of many other levels were refined.

I. INTRODUCTION

The nucleus ^{59}Cu has been extensively studied.[1–35] Lying just beyond the supposed double shell closure at ^{56}Ni, it is an interesting proving ground for that closure. The levels of ^{59}Cu are accessible by a number of reactions, most of which add a proton to ^{58}Ni. Direct (d,n) (Ref. 2), (^{3}He,d) (Refs. 3–9), and (α,t) (Ref. 10) reactions provide the only single particle access. In some cases, particle-gamma[4,8] and particle-particle[7] coincidences and angular correlations have been studied in these reactions. Proton unbound states of ^{59}Cu have been observed in the reactions (d,np) (Ref. 11) and (^{3}He,dp) (Ref. 7) and following the β decay of ^{59}Zn,[12,13] as well as in resonant scattering[14–17] and capture[16,18–35] in the system p + ^{58}Ni. In this way, levels up to 8 MeV excitation have been identified.

Since the levels of ^{59}Ni below 4 MeV are also well-known from both direct and compound nuclear reactions,[1,36–44] it has been possible to identify candidate $T=\frac{3}{2}$ levels in ^{59}Cu by comparing excitation energies, spin-parity values, and single-particle spectroscopic factors between ^{59}Cu and ^{59}Ni. There is a consensus on the selection of analogs of the lowest six ^{59}Ni levels.[5,7,15] Two of these, the $\frac{3}{2}^-$ ground state and the $\frac{3}{2}^-$ 0.878 MeV state of ^{59}Ni, have been observed as close doublets in ^{59}Cu.[7,8,26] The presence of a small analog state splitting in a region of low level density has been attributed to internal mixing with the corresponding antianalog states.[45] A $\frac{9}{2}^+$ level appears at 3.062 MeV in ^{59}Ni. Early searches for its ^{59}Cu analog yielded a single proton capture resonance,[21,22,25] though a second probable fragment was later found nearby.[16] By contrast, the (^{3}He,d) experiments suggest many $l=4$ transitions. The initial phases of the present work confirmed among these the $\frac{9}{2}^+$ nature of the second fragment and identified a third $\frac{9}{2}^+$ state.[34] The relatively large splitting (0.7 MeV) of this proposed analog fragment from the others, compared to the spreading in the lower states, has led to the inclusion of core excitation mechanisms in its formation.[35] The $\frac{9}{2}^+$ resonances of ^{59}Cu are easily distinguished by their $M1$ decay to a bound $\frac{9}{2}^+$ antianalog state. No other resonances in ^{59}Cu are so isolated. Nevertheless, it is of interest to try to identify among the ^{59}Cu levels those which may be analogs of other ^{59}Ni states, and to seek evidence for their splitting. With a larger range of resonances, one may hope to see systematic variations of the Coulomb energy shift and spreading width of analog states with excitation energy and angular momentum.

This paper describes a comprehensive survey of proton capture resonances carried out in the energy range $0.75<E_p<5.0$ MeV ($4.3<E_x<8.3$ MeV). The greatest concentration of effort centered about those groups of resonances which by virtue of their energies were possible analogs of ^{59}Ni levels. The yield curve showed 190 resonances. Singles γ-ray spectra at 56 resonances were used to develop consistent decay schemes and accurate level energies for bound and unbound levels. Gamma-ray angular distributions were measured for 28 resonances, yielding unique spin assignments for 18. Using a γ-decay branching pattern recognition technique,[46] tentative assignments have been made for a further 32 resonances. In addition to the resonance assignments, a number of spin-parity determinations were made for some of the 42 states populated from the resonances. Decay schemes of newly-found bound states were developed and those of many previously studied levels were revised. Propositions for the assignment of a number of new isobaric analog states are made on the basis of energy, spin-parity, and decay properties matching those of states of ^{59}Ni.

Because of the large configuration space involved, it has so far not been possible to carry out shell model calculations for $A=59$ in the complete fp shell. However, only three particles lie outside doubly magic ^{56}Ni. A number of calculations have been made in which the particles have been allowed to occupy the $p_{3/2}$, $f_{5/2}$, and $p_{1/2}$ orbits. For ^{59}Ni there are 37 states for these configurations, about half of which occupy the lowest 3 MeV. Reasonable agreement with experiment has been found.[47–49] These calculations may also be expected to apply to the $T=\frac{3}{2}$ states of ^{59}Cu. However, with the inclusion of $T=\frac{1}{2}$, the number of states becomes very large. Shell model calculations[50,51] have had some success in describing the lowest $T=\frac{1}{2}$ levels. Intermediate coupling models have also proved useful in reproducing the properties of low-lying negative parity levels of the odd Cu isotopes.[52]

II. EXPERIMENTAL PROCEDURE

The experiments were performed at a number of laboratories, as indicated in Table I, and covered the entire range of proton bombarding energies from 0.75 to 5.0 MeV. In most cases the beam energy spread was 1 keV or less. The reliability of the absolute energy calibration varied, but is thought to be within 3 or 4 keV, judging from a comparison of resonance excitation energies calculated from the beam energy and from the decay γ-ray energies. The separation of resonances was found to be reproducible to within 1 keV.

The targets were prepared by vacuum evaporation of enriched ^{58}Ni to a thickness of 20—30 $\mu g/cm^2$ ($\Delta E_p \simeq 1-2$ keV). Target backings of tungsten were carefully selected for low fluorine content and baked before the nickel deposition. This proved to be particularly important at higher bombarding energies. Similar careful attention was paid to the selection and cleaning of the closest beam collimating apertures which were also of tungsten.

For gamma detection, large germanium detectors were used, generally 100—150 cm^3, with resolutions near 2 keV at 1.33 MeV. The efficiency curves were measured using radiations from ^{56}Co sources and the reaction $^{27}Al(p,\gamma)^{28}Si$ at the 0.992 MeV resonance.[53] Energy calibration was obtained using radioactive sources and confirmed in each spectrum using γ rays from identifiable contaminants, notably ^{19}F and ^{27}Al, and room background lines of ^{40}K and ^{228}Th. For the yield curves, a single detector in close geometry at 55° was used (target to detector distance 3—5 cm). The $(p,p'\gamma)$ yield curve was obtained by integrating the 1.453 MeV peak for the $2^+ \to 0^+$ transition in ^{58}Ni and subtracting background sampled on either side of the peak. The yield for the higher energy γ rays was obtained simply from discriminators set at 1.9 and 2.6 MeV. For the angular distributions at selected resonances, the best available detector was placed 7 cm from the target and spectra were measured at 0°, 30°, 45°, 60°, and 90°. A monitor germanium detector was placed at $-90°$. Two independent normalizations were available, in addition to the integrated charge: the intense 1.453 MeV $2^+ \to 0^+$ transition in ^{58}Ni and sometimes intense (p,γ) lines from the monitor counter allowed compensation for small beam energy changes during long angular distribution measurements. Alternatively, the decay of the 0.491 MeV spin-$\frac{1}{2}$ level of ^{59}Cu, when it was sufficiently intense, provided an internal monitor in the moving detector spectrum. This of course has the additional advantage of monitoring solid angle variations. However, it has the disadvantages of low energy and proximity to the 0.511 MeV line.

Spectra taken at 55° and 90° were analyzed by conventional means to obtain γ-ray energies and intensities for all primary and secondary decay branches. In forming the decay scheme for each resonance, attention was paid both to proper energy sums and to intensity balance. The branching percentages presented are thought to have an absolute precision of $\pm 1\%$ or better.

The angular distribution of gamma rays following proton capture on a spin zero target to a resonance of J^π depends only on J, the final state J_f, and the transition multipolarity.[54] A simple analysis of such data is to calculate the best fit distribution for each (J,J_f) combination and to plot the reduced χ^2 against the multipole mixing ratio δ. Whenever it was possible, angular distributions from several primary decay branches to states of known J_f were analyzed independently. In a number of instances, secondary decays were studied as well and their goodness of fit included in the consideration of the primary transition. With the establishment of the resonance spins, it was possible to study angular distributions of transitions to states of unknown J_f.

Where spin measurements were not obtained from angular distributions, often for want of sufficient intensity in two or three decay branches, recourse was made to inference of the spin from the pattern of decay branching, using a statistical method described in detail elsewhere.[46]

TABLE I. List of the experiments.

Measurement	E_p (MeV)	Accelerator	Laboratory
Excitation function	0.75—1.4	3 MeV Van de Graaff	University of Helsinki
Excitation function	1.4—2.5	2.5 MeV Van de Graaff	King Saud University
Excitation function	1.4—3.0	6 MeV Van de Graaff	University of Zürich
Excitation function	3.6—5.0	10 MV Tandem	McMaster University
Angular distributions	1.4—3.6	4 MeV Van de Graaff	Queen's University
Angular distributions	3.48—3.55	7 MeV Van de Graaff	Hahn-Meitner Institüt
Angular distributions	3.6—5.0	10 MV Tandem	McMaster University

TABLE II. Resonances in the system p + ^{58}Ni below $E_p = 5$ MeV

Resonance No.	E_p (MeV)	E_x (MeV)	J^π	Resonance No.	E_p (MeV)	E_x (MeV)	J^π
1	0.949	4.347[a]	$(\frac{1}{2}^-)$	23	2.231	5.608	
2	1.098	4.494		24	2.244	5.620	
3	1.224	4.618		25	2.266	5.642[a]	$(\frac{3}{2},\frac{5}{2})$
4	1.307	4.699[a]	$(\frac{3}{2})$	26	2.282	5.658[b]	$\frac{5}{2}$
5	1.314	4.706		27	2.319	5.694	
6	1.378	4.769[a]	$(\frac{3}{2},\frac{5}{2})$	28	2.337	5.712[a]	$(\frac{5}{2})$
7	1.424	4.814[b]	$\frac{3}{2}$	29	2.344	5.719[b]	$\frac{3}{2},\frac{5}{2}^{(+)}$
8	1.665	5.051[a]	$(\frac{3}{2},\frac{5}{2})$	30	2.428	5.801	
9	1.717	5.102		31	2.449	5.822	
10	1.844	5.227[b]	$\frac{1}{2},\frac{3}{2},\frac{5}{2}$	32	2.460	5.833	
11	1.881	5.264		33	2.479	5.851	
12	1.924	5.306		34	2.509	5.881[b]	$\frac{3}{2},\frac{5}{2}^-$
13	2.051	5.431		35	2.525	5.897[b]	$\frac{7}{2}^+$
14	2.063	5.442		36	2.543	5.914	
15	2.094	5.473		37	2.557	5.928	
16	2.103	5.482		38	2.570	5.941	
17	2.143	5.521[b]	$\frac{3}{2}^-,\frac{5}{2}$	39	2.586	5.957	
18	2.164	5.542		40	2.598	5.968	
19	2.172	5.550[a]	$(\frac{3}{2},\frac{5}{2})$	41	2.601	5.971	
20	2.207	5.584		42	2.664	6.033	
21	2.212	5.589		43	2.670	6.039[b]	$\frac{3}{2}^+$
22	2.225	5.602[a]	$(\frac{3}{2})$	44	2.708	6.076	

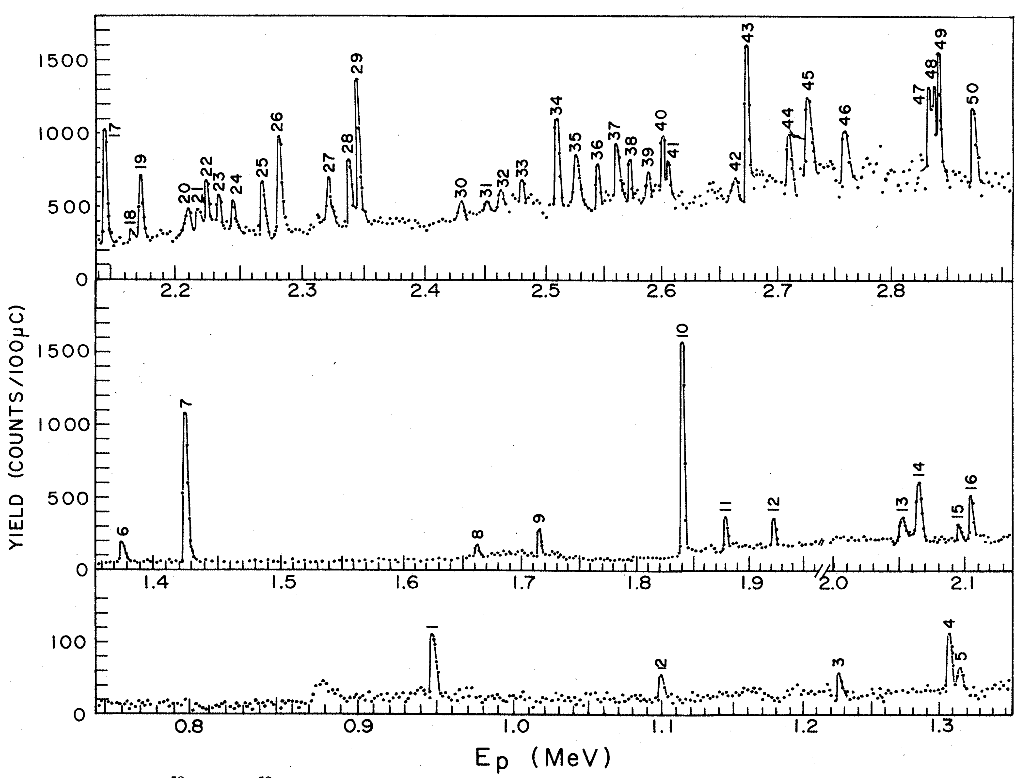

FIG. 1. Yield curve for the ^{58}Ni(p,γ)^{59}Cu reaction for $E_\gamma > 1.9$ MeV, and $0.75 < E_p < 2.9$ MeV. The resonance peaks are numbered. The proton bombarding energy and excitation energy are given in Table II.

TABLE II. (*Continued*).

Resonance No.	E_p (MeV)	E_x (MeV)	J^π
45	2.723	6.091[b]	$\frac{3}{2}^-$
46	2.757	6.125	
47	2.831	6.197[a]	$(\frac{3}{2})$
48	2.835	6.201[a]	$(\frac{3}{2},\frac{5}{2})$
49	2.839	6.206[b]	$\frac{9}{2}^+$
50	2.872	6.238[a]	$(\frac{3}{2},\frac{5}{2})$
51	2.935	6.300[a]	$(\frac{3}{2},\frac{5}{2})$
52	2.958	6.322[a]	$(\frac{5}{2})$
53	2.962	6.326[a]	$(\frac{3}{2})$
54	2.971	6.336	
55	2.976	6.341[a]	$(\frac{3}{2},\frac{5}{2})$
56	2.999	6.362[a]	$(\frac{3}{2})$
57	3.018	6.381	
58	3.032	6.396	
59	3.041	6.404	
60	3.047	6.410	
61	3.056	6.419	
62	3.081	6.444	
63	3.088	6.451	
64	3.095	6.457[b]	$\frac{5}{2}^-$
65	3.099	6.461[b]	$\frac{3}{2}^-$
66	3.108	6.470	
67	3.119	6.481	
68	3.125	6.487	
69	3.131	6.493[b]	$\frac{7}{2}$
70	3.140	6.501	
71	3.149	6.510	
72	3.157	6.519	
73	3.163	6.524	
74	3.171	6.532	
75	3.181	6.542	
76	3.191	6.552	
77	3.199	6.559	

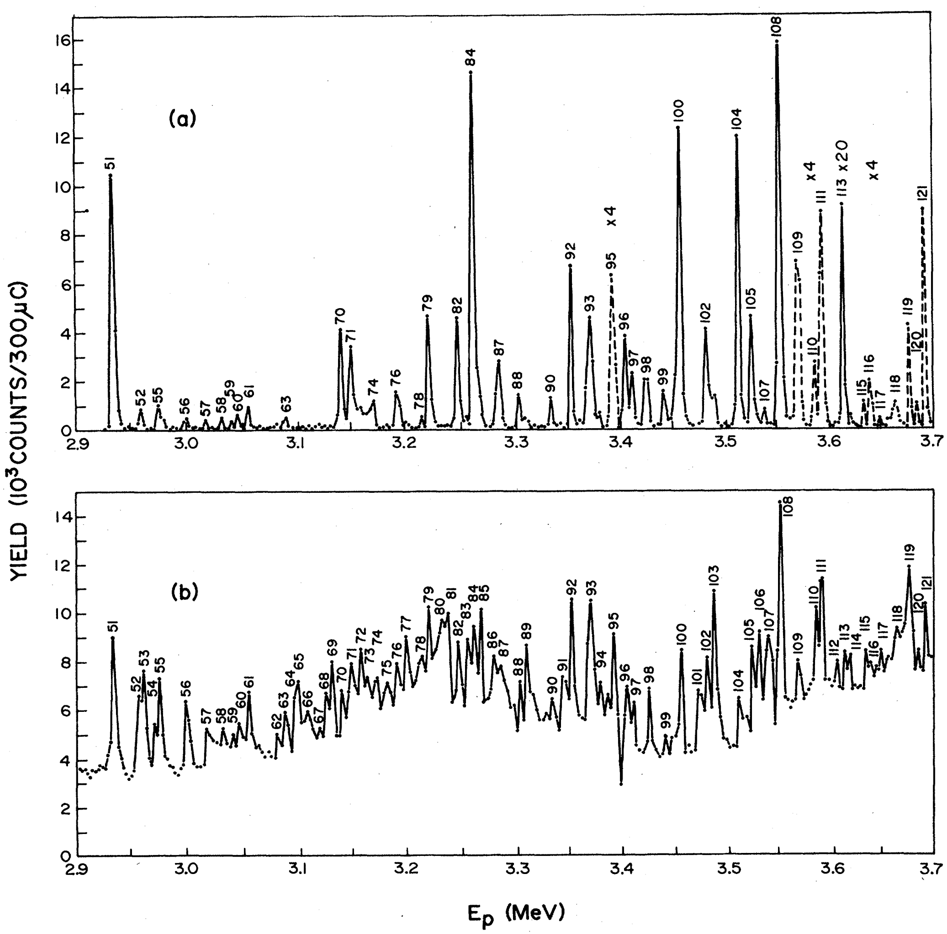

FIG. 2. Yield curves for (a) the $(p,p'\gamma)$ and (b) (p,γ) reactions for $2.9 < E_p < 3.7$ MeV. The inelastic channel was measured by a window on the 1.453 MeV γ ray while the capture channel was selected with a discriminator set at 1.9 MeV. The proton energy and excitation energy are given in Table II. The dashed curves in (a) indicate regions of altered vertical scale.

TABLE II. (*Continued*).

Resonance No.	E_p (MeV)	E_x (MeV)	J^π	Resonance No.	E_p (MeV)	E_x (MeV)	J^π
78	3.212	6.572		100	3.455	6.811	
79	3.220	6.580		101	3.472	6.828	
80	3.231	6.591		102	3.480	6.836[b]	$\frac{9}{2}^+$
81	3.237	6.597		103	3.487	6.843[b]	$\frac{3}{2}^-$
82	3.247	6.607		104	3.511	6.867	
83	3.255	6.615		105	3.524	6.879[a]	$(\frac{5}{2})$
84	3.261	6.621		106	3.530	6.885	
85	3.267	6.627[b]	$\frac{3}{2}$	107	3.539	6.894[b]	$\frac{5}{2}^-$
86	3.279	6.638		108	3.550	6.905[b]	$\frac{9}{2}^+$
87	3.285	6.644		109	3.568	6.923[a]	$(\frac{5}{2})$
88	3.303	6.662		110	3.585	6.939[b]	$\frac{3}{2}^-$
89	3.309	6.668		111	3.591	6.945[a]	$(\frac{3}{2})$
90	3.334	6.692		112	3.605	6.959	
91	3.344	6.702		113	3.613	6.967[a]	$(\frac{3}{2},\frac{5}{2})$
92	3.352	6.710[b]	$\frac{3}{2}$	114	3.618	6.971	
93	3.369	6.727[a]	$(\frac{3}{2},\frac{5}{2})$	115	3.633	6.986	
94	3.379	6.737		116	3.638	6.991	
95	3.391	6.749[b]	$\frac{5}{2}^+$	117	3.648	7.001	
96	3.402	6.760		118	3.663	7.016	
97	3.410	6.768		119	3.676	7.029	
98	3.425	6.782		120	3.683	7.036	
99	3.440	6.797					

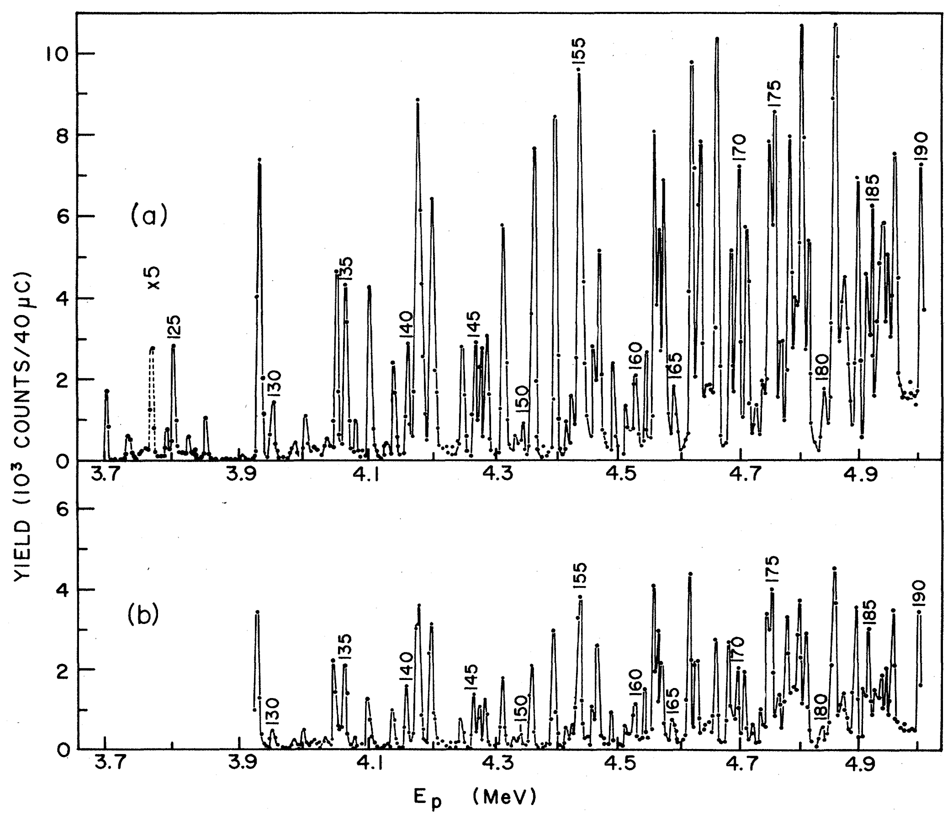

FIG. 3. Yield curve for (p,p′γ) reaction for $3.7 < E_p < 5.0$ MeV at (a) 55° and (b) −90°.

TABLE II. (*Continued*).

Resonance No.	E_p (MeV)	E_x (MeV)	J^π	Resonance No.	E_p (MeV)	E_x (MeV)	J^π
121	3.696	7.048		156	4.455	7.794	
122	3.732	7.083		157	4.462	7.801	
123	3.767	7.117		158	4.486	7.824	
124	3.790	7.140		159	4.505	7.843	
125	3.800	7.150		160	4.525	7.863	
126	3.822	7.172		161	4.539	7.876	
127	3.848	7.197		162	4.553	7.890	
128	3.903	7.251		163	4.560	7.897	
129	3.930	7.278		164	4.567	7.904	
130	3.952	7.299[b]	$\frac{3}{2},\frac{5}{2}$	165	4.585	7.922	
131	3.985	7.332[a]		166	4.614	7.951	
132	4.002	7.348[b]	$\frac{3}{2}^-$	167	4.628	7.964	
133	4.035	7.381		168	4.656	7.991	
134	4.048	7.394[b]	$\frac{5}{2}$	169	4.678	8.013[a]	$(\frac{3}{2})$
135	4.062	7.407[a]		170	4.692	8.027	
136	4.078	7.423		171	4.703	8.038	
137	4.099	7.444[a]	$(\frac{3}{2})$	172	4.721	8.055	
138	4.129	7.473		173	4.732	8.066	
139	4.136	7.480		174	4.743	8.077[b]	$\frac{3}{2}^-,\frac{5}{2}$
140	4.159	7.503		175	4.750	8.084	
141	4.173	7.517[a]	$(\frac{5}{2})$	176	4.762	8.096	
142	4.180	7.523		177	4.775	8.108	
143	4.196	7.539[a]	$(\frac{3}{2})$	178	4.797	8.128	
144	4.244	7.586		179	4.808	8.141	
145	4.265	7.607		180	4.837	8.169	
146	4.275	7.617		181	4.855	8.187	
147	4.282	7.624		182	4.870	8.202	
148	4.309	7.650[b]	$\frac{5}{2}$	183	4.892	8.223[b]	$\frac{3}{2}^-,\frac{5}{2}$
149	4.330	7.671		184	4.906	8.237	
150	4.340	7.681		185	4.914	8.245	
151	4.357	7.697[a]	$(\frac{5}{2})$	186	4.928	8.259[b]	$\frac{3}{2}^-,\frac{5}{2}$
152	4.392	7.732		187	4.936	8.267	
153	4.413	7.752		188	4.943	8.273	
154	4.420	7.759		189	4.954	8.284	
155	4.434	7.773		190	4.999	8.329	

[a]Spectrum measured, spin inferred from decay (Ref. 46).
[b]Angular distribution measured.

III. RESULTS

A. Excitation functions

The yield of the ^{58}Ni(p,γ)^{59}Cu reaction for $E_\gamma > 1.9$ MeV is shown in Fig. 1, for proton energies from 0.75 to 2.90 MeV. For $E_\gamma > 2.6$ MeV, the excitation function is quite similar. No resonance was found below 0.949 MeV, the analog of the 0.465 MeV $\frac{1}{2}^-$ level of ^{59}Ni. The analogs of the ground $(\frac{3}{2}^-)$ and 0.339 MeV $(\frac{5}{2}^-)$ levels are also proton unbound and would appear at proton energies of 0.49 and 0.90 MeV, respectively. However, their cross sections are expected to be very small because of low penetrability of the Coulomb and centrifugal barrier.

The increase of level density with energy is obvious in Fig. 1. Up to No. 19, at 2.17 MeV, the resonances are well separated. Above this, there are a number of close multiplets (e.g., 40-41 and 47-48-49). The last of these resonances, No. 49, shows characteristics similar to those of the established $g_{9/2}$ isobaric analog states (IAS). It will be discussed further in the following.

Figure 2 shows the yield curves for the (p,γ) and (p,p'γ) reactions for proton energies from 2.9 to 3.7 MeV. Above 3 MeV, the average resonance spacing remains almost

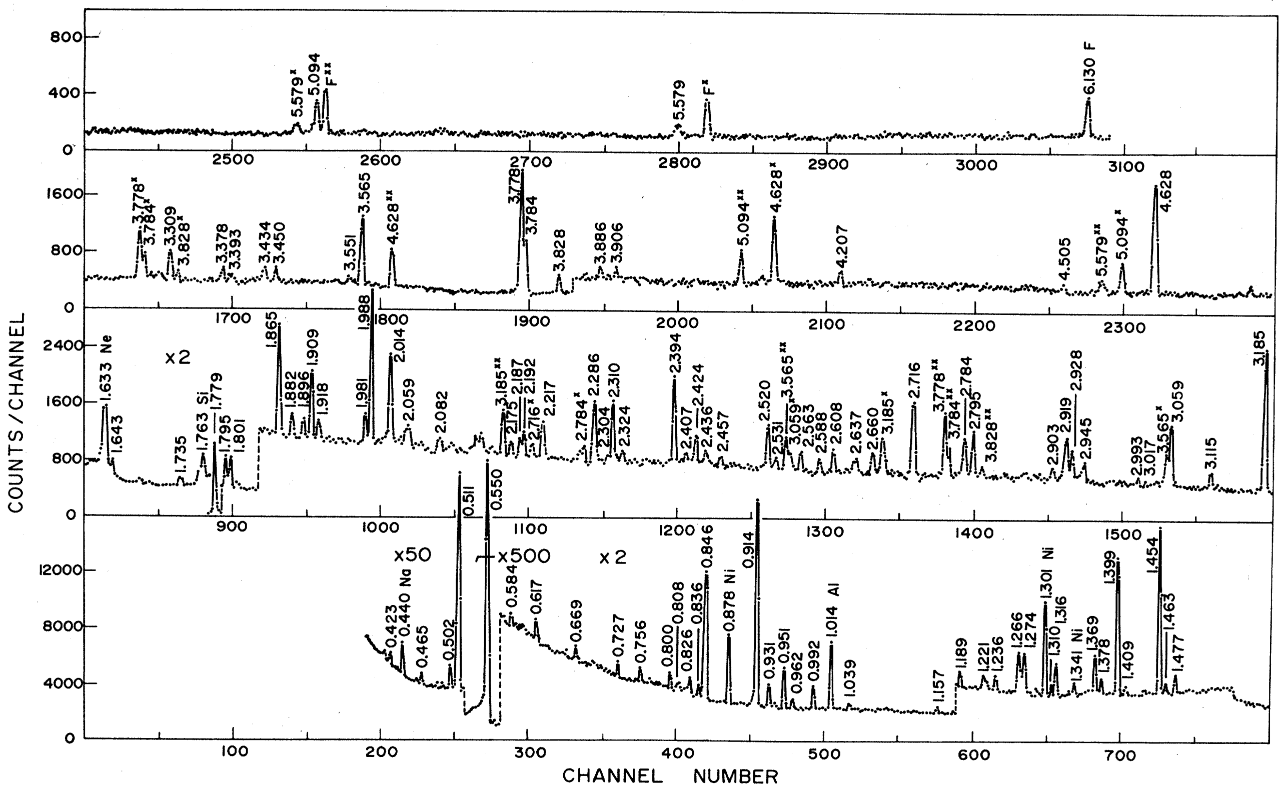

FIG. 4. Spectrum of γ rays at resonance No. 69, $E_p = 3.131$ MeV. The spectrum shows 34 primary transitions which populate levels up to 4.307 MeV.

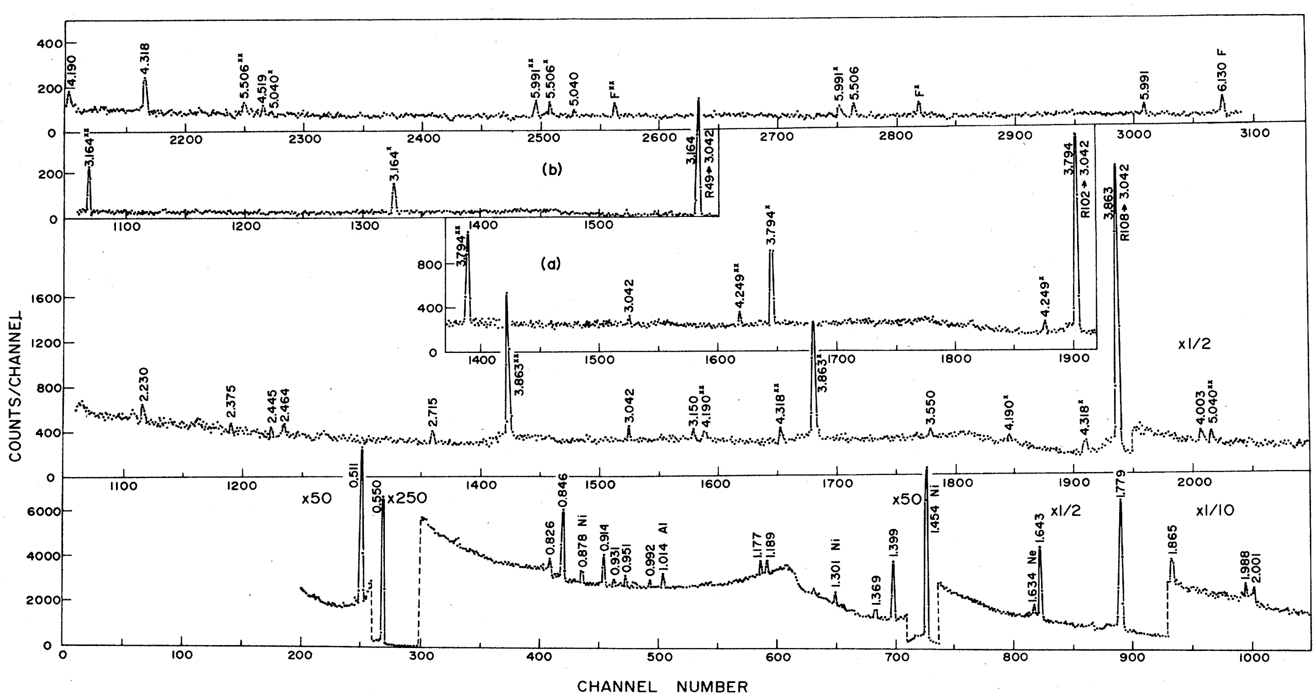

FIG. 5. Spectrum of the 3.550 MeV $\frac{9}{2}^+$ resonance, No. 108, with insets (a) and (b) showing the principal decays of the 3.480 and 2.839 MeV resonances (102 and 49), respectively.

TABLE III. Decay branching ratios (%) for ^{59}Cu resonances.

Resonance No. / E_f (MeV)	1	4	6	7	8	10	17	19	22	25	26	28	29	34	35	43	45	47
0.0	6	63	3	27	30	86	89	37	50	30		56	13	70		46	70	
0.491	16	21	36	55		6			13	12			3	6		12	15	39
0.914			19	5	15		6		3	18	13	7		3		9		
1.399							4			4	43	10			88			
1.865			3					23		2	3							
1.988			11	7	36					2	5		35	4	6	8		
2.266	17		8	2		6		17	11	10	8	7				7		8
2.318	9		7						10	7	3		15	13				
2.324	27	16		3						3			22			9	11	23
2.587																		
2.664																		
2.709			2		3													
2.716			1		7		1				12	4		3		2		8
2.928			2					7			2		7			2		
2.993										7								
3.024	8					1			13		1		5				3	
3.042																		
3.115					9			4		3		4			6			
3.130	17		2															
3.309																		
3.434				1				1				4						
3.438			4	<1		1		3										
3.551											1					<1		
3.574																		
3.578											3	6				4	1	22
3.615								5			5							
3.699										2				1		1		
3.729																		
3.742			2					3				2						

TABLE III. (*Continued*).

Resonance No. E_f (MeV)	48	49	50	51	52	53	55	56	64	65	69	85	92	93	95	102	103	105
0.0	5		34	9	8	65	7	35	6.5	4.5		77.2	37.0	78.0	88.3		56.3	19.3
0.491	13		28	22	13	5	7	40		13.3		4.1	49.0	5.5			31.1	
0.914	6				5		46	14	39.0	25.3	2.6						5.0	31.3
1.399			14		9				4.4		4.6			2.4	4.2	19.9		13.6
1.865				5	45	12					8.9							
1.988	21	4	4	18					3.8	2.5	0.4							
2.266	5		7	4	4	12	18			5.5			3.4				3.2	
2.318				5	11	6				12.4		5.4	1.0					
2.324	18								6.2	11.6		4.9	1.7	3.2	2.9		4.4	7.4
2.587		6														12.1		
2.664											2.2							
2.709	4			2				3	11.9	6.8	6.2							6.1
2.716		3		5	5		7			16.1				2.7		1.3		
2.928	4			20					1.1		7.2	2.1	2.7					
2.993							3		2.7									13.7
3.024	5		4				1			3.0								
3.042		84									1.7					64.9		
3.115	13	3		8					1.7		1.5							4.2
3.130									1.4	7.4			2.5					
3.309											14.5							
3.434									1.7		6.4	1.3						
3.438	6								1.2				2.7					
3.551							8		1.5		1.9							
3.574									6.7		4.4							
3.578			9				3	8		4.5		5.0		4.0	2.3			4.4
3.615				2						1.9								
3.699							<1		4.7		3.7							
3.729																		
3.742																		
3.756																		
3.887											1.8			2.3	2.3			
3.906											1.1			1.9				
3.930											1.3							
4.072											2.2							
4.183											3.9							
4.207											4.9							
4.301											1.2							
4.307											1.3							
4.441																		
4.465																		
4.530																1.8		
4.917																		

TABLE III. (*Continued*).

Resonance No. E_f (MeV)	107	108	109	110	111	113	130	131	132	134	135	137	141	143	148	151	169
0.0	11.0			7.7	45.6	57.6	72	100	68	7	100	70	30	25	60	38	67
0.491				13.3	10.6									55			33
0.914	11.2	2.6	38.2	8.6		24.3	8		12					20			
1.399	20.0	3.5											70		40	18	
1.865		1.1		5.7						8						17	
1.988	14.2		46.0			6.3	6			13						10	
2.266	13.0			22.2	23.7	5.9	6										
2.318				3.7	13.0												
2.324	10.6			9.8	7.1												
2.587		6.7															
2.664																	
2.709	5.0																
2.716	6.0	2.7		8.0													
2.928																	
2.993				4.7													
3.024																	
3.042		76.1															
3.115	3.5																
3.130						2.0	8										
3.309																	
3.434																	
3.438																	
3.551	5.5																
3.574																	
3.578			15.8			3.9			20	72		15					
3.615												15					
3.699																	
3.729				16.3													
3.742																	
3.756		1.5															
3.887																	
3.906																	
3.930																	
4.072																	
4.183																	
4.207																	
4.301																	
4.307																	
4.441		2.0															
4.465		0.9															
4.530		1.1															
4.917		1.8															

constant at 15 keV. In this region two groups of resonances are of particular interest. In the first, resonances 64, 65, and 69 provide abundant spectroscopic information on bound states. Resonance 108 is the well-studied $g_{9/2}$ IAS while 102 is its less familiar companion. In Fig. 2(a), the rapid rise of the (p,p$'\gamma$) yield may be seen. Although the background is low, the average spacing remains at 15 keV, suggesting that the observations are limited by resolution.

In Fig. 3, the inelastic yield curve is continued up to 5 MeV. It is very dense, but the correlation between yields at two angles gives some confidence in the assignment of energies to resonances, many of which are undoubtedly unresolved multiplets. Some of the resonances were selected for study of spectra and γ-ray angular distributions in the capture channel because (^{3}He,d) measurements[7] had suggested large single particle strength.

B. Resonance decay schemes

At each of the resonances indicated with an "a" in Table II, a spectrum was acquired with a detector placed at 55° in close geometry for an integrated beam charge of 10—50 mC depending on the intensity of the resonance. A typical spectrum, taken at the 3.131 MeV resonance (No. 69), is shown in Fig. 4. Prominent impurity lines from the (p,p$'\gamma$) reaction are 0.440 MeV from ^{23}Na; 0.846 and 1.014 MeV from ^{27}Al; and 1.779 and 1.982 MeV from ^{28}Si and ^{18}O, respectively. Lines at 1.633 and 6.129 MeV are from (p,$\alpha\gamma$) reactions on ^{23}Na and ^{19}F, respectively.

TABLE IV. Decay branching ratios (%) for ^{59}Cu bound states.

E_i	E_f (MeV)							
(MeV)	0	0.491	0.914	1.399	1.865	1.988	2.324	2.709
0.491	100							
0.914	100							
1.399	100							
1.865	30		55	15				
1.988	100							
2.266	52	48						
2.318	83	17						
2.324	90		10					
2.587				100				
2.664					100			
2.709		27	59	14				
2.716	37		28	20		15		
2.928	34	10	45			11		
2.993	37		58			5		
3.024	45	40	15					
3.042	1		3	76	20			
3.115	72	28						
3.130	29	35	36					
3.309	25		45	30				
3.434	30		70					
3.438	100							
3.551	35		65					
3.574			70	30				
3.578	34		33		33			
3.615	35	65						
3.699			100					
3.729				25		35	45	
3.742			50			50		
3.756			60	40				
3.887	45					55		
3.906	50		50					
3.930			25	75				
4.072			25			75		
4.183				40				60
4.207	24		28	22			26	
4.301			40	60				
4.307			100					
4.441			50	50				
4.465			100					
4.530			100					
4.917			100					

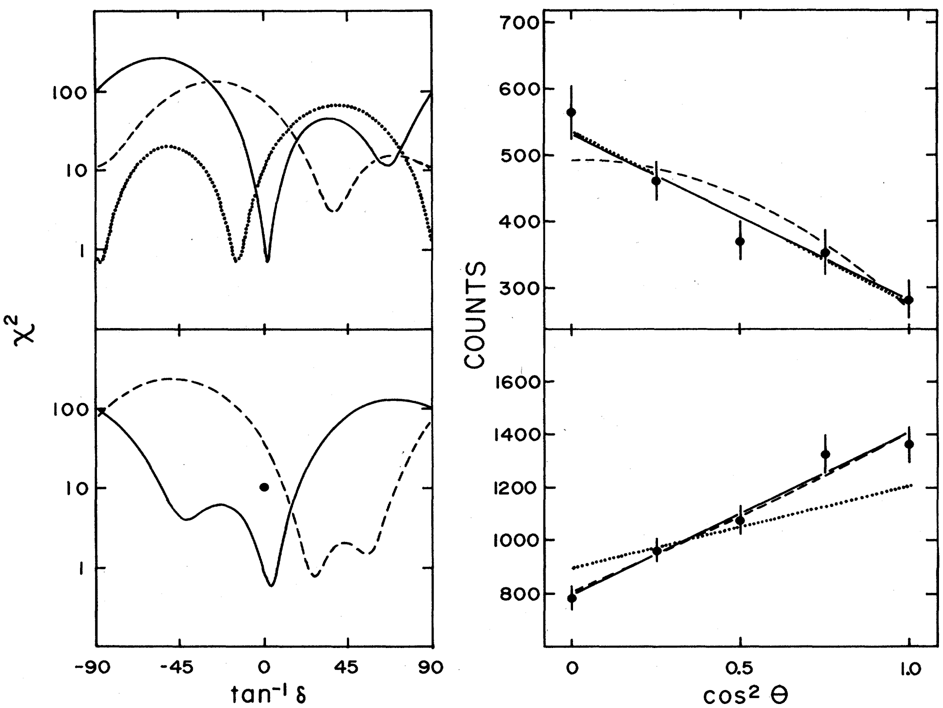

FIG. 6. Analysis of angular distributions of two primary decays from the 3.131 MeV resonance. The solid curves are for $J=\frac{7}{2}$, dashed for $J=\frac{5}{2}$, and dotted for $J=\frac{3}{2}$. On the left-hand side are plots of χ^2 against $\tan^{-1}\delta$ and on the right-hand side the corresponding angular distribution fits at minimum χ^2. Upper: $R\,69\rightarrow2.709$, $J_f=\frac{5}{2}$; lower: $R\,69\rightarrow2.716$, $J_f=\frac{7}{2}$.

These lines, while producing unwanted background in the (p,γ) spectra, did provide convenient detector calibration.

Some of the resonances are particularly rich in decay branches. For instance, the three resonances at $E_p=3.095$, 3.099, and 3.131 MeV together populate 37 of the 42 bound states. The γ-ray spectrum measured at $E_p=3.131$ MeV is shown in Fig. 4. There are 23 primary transitions with energies from 5.579 to 2.187 MeV, including a number of close doublets. The pair of levels at 2.709-2.716 MeV is fed by the γ rays 3.784-3.778 MeV. The transitions at $E_\gamma=2.587$-2.606 MeV populate levels at 3.906-3.887 MeV, while those at $E_\gamma=2.187$-2.192 MeV populate levels at 4.307-4.301 MeV, as shown in Fig. 8. A further transition of some interest from this resonance is to the $\frac{9}{2}^+$ level at 3.042 MeV. The only other resonances which feed this state are those at $E_p=2.839$, 3.480, and 3.550 MeV. These, however, show comparatively simple decay schemes, with the $\frac{9}{2}^+$ state dominating. The spectrum of the 3.550 MeV resonance (No. 108) is shown in Fig. 5. The insets (a) and (b) show only the strong transition to the 3.042 MeV level for the other two resonances. Table III contains the decay branching ratios for all the resonances studied. Forty-two states of ^{59}Cu up to an excitation energy of 4.917 MeV were populated.

The decay scheme of bound states of ^{59}Cu, established from secondary transitions following resonance capture are given in Table IV. For most of the levels, spectra at several resonances were used to determine the branching ratios.

C. Gamma-ray angular distributions, J^π for resonances and bound states

Angular distributions were measured at the 28 resonances indicated with a "b" in Table II. Figures 6 and 7 are examples of the analyses. The measured angular distribution coefficients, and their interpretation in terms of initial and final state spins J_i and J_f, and the quadrupole to dipole amplitude mixing ratio δ (phase convention of Rose and Brink[55]), are listed in Table V. The only J_f^π values presumed at the outset were taken from Ref. 1. They are $(E_x,J^\pi)=(0,\frac{3}{2}^-)$, $(0.491,\frac{1}{2}^-)$, $(0.914,\frac{5}{2}^-)$, $(1.399,\frac{7}{2}^-)$, $(1.865,\frac{7}{2})$, $(1.988,\frac{5}{2})$, $(2.266,\frac{3}{2}^+)$, $(2.324,\frac{3}{2})$, $(2.709,\frac{5}{2})$, $(2.716,\frac{7}{2})$, $(3.042,\frac{9}{2}^+)$, and $(3.578,\frac{5}{2}^+)$. The spin and parity ambiguities in the above-mentioned list will be discussed in the following. In arriving at the choice of spin for each resonance, only values resulting in a reduced $\chi^2_{\min}>5.4$ (0.1% confidence level for a five-angle distribution) were rejected. Of course the angular distributions do not establish the parity of the transition $\pi_i\pi_f$. Since no linear polarization measurements were made, determination of the parity of the transitions must rest on model-dependent arguments. Most of the observed resonances have total radiative widths between 0.1 and 1 eV,[19] considerably smaller than the single particle widths for $E1$ and $M1$ transitions, which are near 200 and 5 eV, respectively, at $E_\gamma=6$ MeV. Consequently, only those transitions with appreciable quadrupole content may be taken to indicate parity. As a working rule, it has been

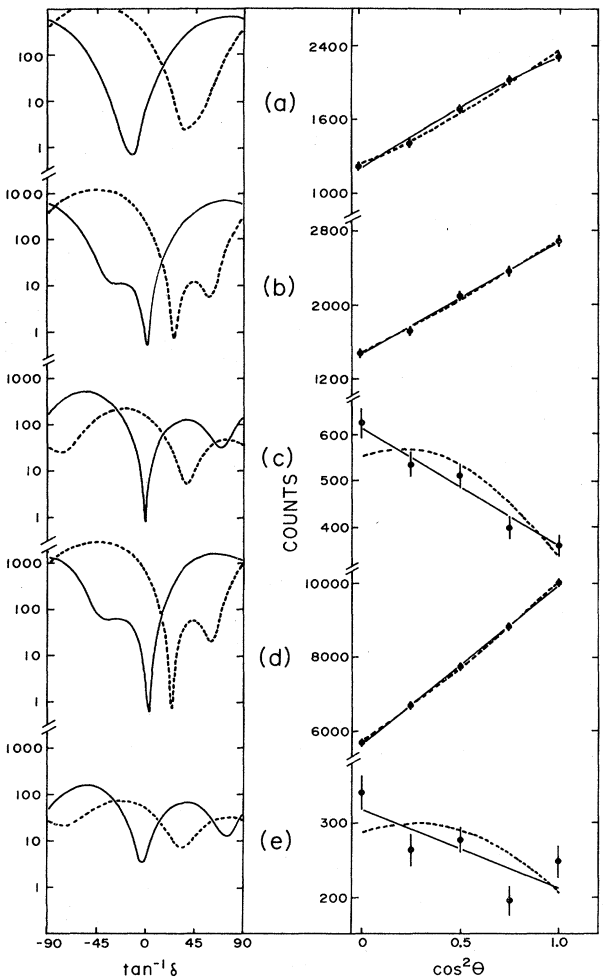

FIG. 7. Analysis of angular distributions of primary decays from the $\frac{9}{2}^+$ states. On the left-hand side are shown the χ^2 plots and on the right-hand side the corresponding angular distribution fits. (a) $R\,49\to3.042$ MeV ($J_f=\frac{9}{2}$), (b) $R\,102\to3.042$ MeV, (c) $R\,102\to1.399$ MeV ($J_f=\frac{7}{2}$), (d) $R\,108\to3.042$ MeV, (e) $R\,108\to1.399$ MeV. Solid lines: $J=\frac{9}{2}$; broken lines: $J=\frac{7}{2}$.

assumed here that the appearance of more than 5% quadrupole intensity indicates a transition with no parity change. Further restrictions of the possible spins and parities may be made by considering the branching to other bound levels. When this has been done in order to reach a value entered in Table II, mention is made in the following, in the form of footnotes to Table V.

Two examples illustrate the process of analysis. In Fig. 6, two decays of resonance 69, at $E_p=3.131$ MeV, are considered. The decay to the spin-$\frac{5}{2}$ level at 2.709 MeV allows spin $\frac{3}{2}$ and $\frac{7}{2}$ and almost rejects $\frac{5}{2}$, while the second transition, to the $\frac{7}{2}^-$ 2.716 MeV level, rejects $\frac{3}{2}$. The $\frac{5}{2}$ option requires an appreciable quadrupole content, and hence a $\frac{5}{2}^-$ resonance spin-parity assignment. This, however, is inconsistent with the decay branch to the $\frac{9}{2}^+$ 3.042 MeV level, discussed in Sec. III B. We are thus led to the conclusion that the resonance spin is $\frac{7}{2}$, but not to the knowledge of the parity, since the transitions are dipolar. Figure 7 shows the angular distributions for decays from resonances 49, 102, and 108. Parts (a), (b), and (d), in which the major decay branch to the $\frac{9}{2}^+$ final state is considered, demonstrate a well-known ambiguity between $\frac{9}{2}$(dipole)$\frac{9}{2}$ and $\frac{7}{2}$(dipole + quadrupole)$\frac{9}{2}$ interpretations. Part (c) shows the rejection of spin $\frac{7}{2}$ for resonance 102, where a second branch to a $\frac{7}{2}^-$ level is fairly intense. For resonance 108, this transition is weaker, giving poorer rejection in (e). At resonance 49, the corresponding transition was too weak. In each case, the selection of resonance spin $\frac{9}{2}$ requires nearly dipole transitions, whereas $\frac{7}{2}$ requires considerable quadrupole content. Since the final state spin parity is $\frac{9}{2}^+$, the initial states must have $J_i^\pi=\frac{9}{2}^\pm$ or $\frac{7}{2}^+$. On the other hand, the measured decays to $\frac{7}{2}^-$ states allow $\frac{9}{2}^\pm$ or $\frac{7}{2}^-$.

With the establishment of these J^π values for the resonances, a number of assignments to bound and nearly bound states become possible. These are shown in Table VI. The spin values attributed to resonances on the basis of the statistical analysis of decay branching[46] are shown in parentheses in Table II. They do not depend on, nor were they used in the bound state determinations.

TABLE V. Results of the angular distribution measurements.

Resonance No.	E_i (MeV)	E_f (MeV)	A_2	A_4	J_i	J_f	δ	χ^2
7	4.814	0	0.47(2)	0.04(3)	$\frac{3}{2}$	$\frac{3}{2}$	−0.05(5), −3.3(7)	1
		0.491	−0.48(2)	0.03(2)		$\frac{1}{2}$	−0.04(4), 1.8(7)	1.5
10	5.227	0	0.01(2)	−0.01(2)	$\frac{1}{2}$	$\frac{3}{2}$		0.5
					$\frac{3}{2}$		0.25(4), >20	0.1
					$\frac{5}{2}$		−0.20(4)	2[a]
17	5.521	0	−0.51(2)	0.04(2)	$\frac{3}{2}$	$\frac{3}{2}$	0.73(5), 2.6(2)	5
					$\frac{5}{2}$		0.04(2)	5
26	5.658	1.399	−0.19(4)	0.01(4)	$\frac{5}{2}$	$\frac{7}{2}$	−0.03(5)	0.6
					$\frac{9}{2}$		−0.07(4)	0.6[b]

TABLE V. (*Continued*).

Resonance No.	E_i (MeV)	E_f (MeV)	A_2	A_4	J_i	J_f	δ	χ^2
29	5.719	0	0.04(5)	0.01(7)	$\frac{3}{2}$	$\frac{3}{2}$	0.23(6), > 7	0.1
					$\frac{5}{2}$		−0.21(18)	0.1
		1.988	−0.02(6)	0.04(7)	$\frac{3}{2}$	$\frac{5}{2}$	0.09(9)	2[c]
					$\frac{5}{2}$		0.37(10)	1
34	5.881	0	0.40(9)	0.09(9)	$\frac{3}{2}$	$\frac{3}{2}$	0.0(1), < −3	0.3
					$\frac{5}{2}$		−0.4(1)	0.1
35	5.897	1.399	0.43(5)	−0.08(7)	$\frac{7}{2}$	$\frac{7}{2}$	0.07(10)	0.7
		1.988	−0.68(23)	0.34(4)		$\frac{5}{2}$	2.5(11)	1
		3.115	−0.72(20)	0.23(19)		$\frac{5}{2}$	0.1(11)	1
43	6.039	0	0.11(4)	0.02(4)	$\frac{3}{2}$	$\frac{3}{2}$	0.17(4), > 10	0.4
		0.491	−0.61(17)	0.09(16)		$\frac{1}{2}$	0.05(8), 1.5(3)	0.3
		0.914	−0.09(15)	−0.14(16)		$\frac{5}{2}$	−0.06(11), > 4	1
		1.988	0.24(15)	0.13(16)		$\frac{5}{2}$	1.0(7)	1
		2.266	−0.74(21)	0.10(19)		$\frac{3}{2}$	1.5(7)	0.8
		2.324	0.48(16)	−0.13(18)		$\frac{3}{2}$	−0.03(11), > 3	0.7
		3.578	−0.56(16)	−0.16(16)		$\frac{5}{2}$	−0.65(22), −4(2)	1
45	6.091	0	−0.01(4)	−0.07(4)	$\frac{3}{2}$	$\frac{3}{2}$	0.29(4), > 14	2.5
		0.491	0.24(23)	0.10(24)		$\frac{1}{2}$	0.4(2), > 3	0.2
		2.324	−0.21(15)	−0.11(24)		$\frac{3}{2}$	0.5(1),6(2)	0.6
49	6.206	1.988	−0.34(15)	0.26(21)	$\frac{9}{2}$	$\frac{5}{2}$		8
		2.587	0.03(17)	−0.18(19)		$\frac{11}{2}$	0.10(15)	1.3
		3.042	0.59(12)	−0.01(13)		$\frac{9}{2}$	−0.3(4)	0.1[d]
64	6.457	0.914	0.36(7)	−0.04(10)	$\frac{5}{2}$	$\frac{5}{2}$	0.09(12)	0.3
		1.399	−0.67(19)	−0.10(19)		$\frac{7}{2}$	< −0.27	0.6
		2.324	−0.83(14)	0.16(15)		$\frac{3}{2}$	0.2(1)	0.4
		2.709	0.49(7)	−0.07(10)		$\frac{5}{2}$	0.0(1), 1.3(3)	1
		2.993	−0.38(19)	0.06(21)		$\frac{3}{2}$	0.0(2)	0.1
						$\frac{5}{2}$	0.9(5), > 6	0.4
						$\frac{7}{2}$	−0.2(2), > 6	0.1
		3.574	0.07(13)	0.11(14)		$\frac{5}{2}$	0.2(2)	0.4
						$\frac{7}{2}$	0.2(1),4(2)	0.2
		3.699	0.40(13)	0.00(14)		$\frac{7}{2}$	1.4(12)	0.2
		4.301	0.05(13)	0.12(15)		$\frac{5}{2}$	0.3(2)	0.5
						$\frac{7}{2}$	0.2(2), > 2	0.3

TABLE V. (*Continued*).

Resonance No.	E_i (MeV)	E_f (MeV)	A_2	A_4	J_i J_f	δ	χ^2
65	6.461	0.491	0.89(21)	−0.09(19)	$\frac{3}{2}$ $\frac{1}{2}$	0.6(2)	0.4
		0.914	−0.05(16)	0.02(19)	$\frac{5}{2}$	0.05(14),4.7(25)	0.1
		2.266	−0.28(14)	0.15(14)	$\frac{3}{2}$	0.4(1)	1.5
		2.318	−0.92(15)	0.03(16)	$\frac{1}{2}$	0.3(1),0.9(1)	2
					$\frac{5}{2}$	−1.3(4)	3
		2.324	0.64(19)	0.01(22)	$\frac{3}{2}$	0.2(11), −2.4(9)	1.5
		3.024	−0.36(29)	0.00(31)	$\frac{5}{2}$	−0.2(2), > 5	0.1
		3.130	0.48(14)	0.13(14)	$\frac{1}{2}$	0.5(1), > 10	1
					$\frac{3}{2}$	0.0(1), > 4(1)	1
					$\frac{5}{2}$	0.9(4), > 4.7	1
		3.578	−0.47(18)	−0.14(18)	$\frac{5}{2}$	−0.4(2), −11(8)	0.7
		3.615	−0.28(29)	0.13(30)	$\frac{3}{2}$	0.5(2), > 2.6	0.2
					$\frac{5}{2}$	−0.1(2), > 3	0.2
69	6.493	1.399	0.40(8)	−0.02(8)	$\frac{7}{2}$ $\frac{7}{2}$	0.1(1)	0.8
		1.865	0.32(6)	0.03(7)	$\frac{7}{2}$	0.15(8)	0.4
		2.664	0.52(15)	−0.15(15)	$\frac{5}{2}$	0.4(2)	2
					$\frac{7}{2}$	0.8(6)	1.5
					$\frac{9}{2}$	1.2(9)	2
					$\frac{11}{2}$	1(1)	2
		2.709	−0.45(8)	0.09(8)	$\frac{5}{2}$	0.03(5)	0.7
		2.716	0.43(5)	−0.03(7)	$\frac{7}{2}$	0.05(11)	1
		2.928	−0.42(6)	−0.03(7)	$\frac{5}{2}$	0.9(2)	3
		3.042	−0.15(20)	−0.19(21)	$\frac{9}{2}$	−0.05(16)	0.5
		3.115	−0.24(22)	−0.07(23)	$\frac{5}{2}$	0.0(2)	0.1
		3.309	0.31(4)	−0.01(4)	$\frac{7}{2}$	0.16(6)	1
		3.434	−0.28(8)	−0.12(9)	$\frac{5}{2}$	0.00(4)	1
		3.574	0.69(12)	−0.20(12)	$\frac{5}{2}$	−0.5(1)	1
					$\frac{7}{2}$	−0.4(6)	1
		3.699	0.00(11)	−0.10(11)	$\frac{7}{2}$	0.5(2)	0.5
		3.887	0.93(25)	−0.23(26)	$\frac{3}{2}$		2
					$\frac{5}{2}$	−0.8(4)	1
		3.906	0.39(18)	−0.18(19)	$\frac{3}{2}$		0.4
					$\frac{5}{2}$	0.3(1)	0.6
					$\frac{7}{2}$	1.4(7)	0.3
		3.930	−0.31(27)	−0.20(27)	$\frac{5}{2}$	0.0(2)	0.3
					$\frac{7}{2}$	> 0.5	0.1
		4.072	0.52(24)	−0.02(26)	$\frac{3}{2}$		0.8
					$\frac{5}{2}$	−0.4(2)	0.1
					$\frac{7}{2}$	−0.6(8)	0.1
					$\frac{9}{2}$	> 0.2	0.1
					$\frac{11}{2}$		0.6

TABLE V. (*Continued*).

Resonance No.	E_i (MeV)	E_f (MeV)	A_2	A_4	J_i J_f	δ	χ^2
		4.183	−0.05(10)	−0.10(10)	$\frac{5}{2}$	−0.1(1)	0.4
					$\frac{7}{2}$	0.6(2)	0.3
					$\frac{9}{2}$	0.03(8)	2
		4.207	−0.26(8)	0.01(10)	$\frac{5}{2}$	−0.04(5)	0.1
					$\frac{7}{2}$	0.7(2)	1
		4.301	−0.02(17)	−0.18(19)	$\frac{5}{2}$	−0.1(1)	0.9
					$\frac{7}{2}$	0.6(2), −3.7(20)	1
		4.307	0.02(17)	−0.33(18)	$\frac{5}{2}$	−0.1(1)	2.5
85	6.627	0	0.37(2)	−0.02(2)	$\frac{3}{2}$ $\frac{3}{2}$	0.03(3), <3.6	3
		3.578	−0.42(11)	−0.02(12)	$\frac{5}{2}$	−0.2(1)	0.8
92	6.710	0	0.38(3)	−0.02(3)	$\frac{3}{2}$ $\frac{3}{2}$	0.02(3),4(1)	0.2
		0.491	−0.78(2)	0.01(2)	$\frac{1}{2}$	0.16(4), 1.1(1)	2
95	6.749	0	0.02(2)	0.04(2)	$\frac{5}{2}$ $\frac{3}{2}$	−0.21(3)	8
		1.399	−0.25(5)	0.15(5)	$\frac{7}{2}$	−0.05(2)	10
		3.578	0.71(12)	−0.74(22)	$\frac{5}{2}$	−2(1)	4
		3.742	−0.57(24)	0.22(26)	$\frac{3}{2}$	0.04(13), 1.8(4)	2
					$\frac{5}{2}$	0.8(2)	3
					$\frac{7}{2}$	−0.3(2), < −2	2
		3.887	0.03(13)	−0.30(14)	$\frac{3}{2}$	−0.1(1)	3
					$\frac{5}{2}$	0.5(2), < −3	2
102	6.836	1.399	−0.36(5)	0.01(5)	$\frac{9}{2}$ $\frac{7}{2}$	0.00(5)	0.8
		2.587	−0.35(12)	0.22(13)	$\frac{11}{2}$	0.0(1)	2
		3.042	0.46(3)	0.01(3)	$\frac{9}{2}$	0.02(7)	0.5[d]
103	6.843	0	−0.20(2)	−0.01(2)	$\frac{3}{2}$ $\frac{3}{2}$	0.4(1),7(2)	0.3
		0.491	−0.02(3)	0.00(3)	$\frac{1}{2}$	−0.3(1),4(1)	1
107	6.894	0.914	−0.15(14)	−0.14(15)	$\frac{5}{2}$ $\frac{5}{2}$	0.6(3), < −3	0.3
		1.399	0.43(5)	0.18(7)	$\frac{7}{2}$	1.4(11)	1
		1.988	0.17(14)	0.00(15)	$\frac{5}{2}$	0.2(2)	0.2
		2.266	0.56(18)	0.08(19)	$\frac{3}{2}$	−0.5(2)	0.3
		2.324	−0.42(17)	−0.10(18)	$\frac{3}{2}$	0.04(12)	0.2
		3.551	−0.26(19)	0.32(20)	$\frac{5}{2}$	0.5(3)	2
108	6.905	1.399	−0.32(8)	0.14(8)	$\frac{9}{2}$ $\frac{7}{2}$	−0.04(6)	3.5
		2.587	−0.12(6)	0.04(7)	$\frac{11}{2}$	0.05(7)	0.2
		2.716	−0.24(13)	0.08(13)	$\frac{7}{2}$	0.06(8)	1
		3.042	0.42(1)	0.01(2)	$\frac{9}{2}$	0.07(5)	0.5[d]
		4.441	−0.48(18)	0.09(20)	$\frac{7}{2}$	0.04(8)	2
					$\frac{11}{2}$	−0.2(2)	2

TABLE V. (*Continued*).

Resonance No.	E_i (MeV)	E_f (MeV)	A_2	A_4	J_i	J_f	δ	χ^2
110	6.939	0.491	−0.01(13)	−0.04(13)	$\frac{3}{2}$	$\frac{1}{2}$	−0.25(11),4(2)	0.6
		0.914	−0.71(20)	0.03(20)		$\frac{5}{2}$	< -0.3	0.8
		2.266	0.12(7)	0.11(8)		$\frac{3}{2}$	0.2(1), < -7	1
		3.729	−0.03(4)	−0.02(5)		$\frac{3}{2}$	0.30(5), > 10	1
						$\frac{5}{2}$	0.06(8),4(1)	1
130	7.299	0	0.07(4)	−0.01(5)	$\frac{3}{2}$	$\frac{3}{2}$	0.21(5), < -10	0.5
					$\frac{5}{2}$		−0.21(4)	0.7
132	7.348	0	−0.24(8)	0.12(11)	$\frac{3}{2}$	$\frac{3}{2}$	0.5(1),6(3)	0.7
					$\frac{5}{2}$		−0.06(5)	0.7
134	7.394	3.578	0.57(6)	0.00(8)	$\frac{5}{2}$	$\frac{5}{2}$	−0.1(1)	3
					$\frac{7}{2}$		−0.5(1)	3[e]
148	7.650	0	−0.63(5)	0.13(3)	$\frac{5}{2}$	$\frac{3}{2}$	0.1(1)	12
		1.399	−0.75(7)	−0.04(8)		$\frac{7}{2}$	−0.1(1)	5
174	8.077	0	−0.59(4)	0.03(3)	$\frac{3}{2}$	$\frac{3}{2}$	1.0(2),1.7(3)	1
					$\frac{5}{2}$		0.09(2)	0.6
183	8.223	0	−0.56(3)	0.01(3)	$\frac{3}{2}$	$\frac{3}{2}$	0.9(2),1.8(3)	0.2
					$\frac{5}{2}$		0.07(3)	0.4
186	8.259	0	−0.43(15)	0.02(4)	$\frac{3}{2}$	$\frac{3}{2}$	0.65(5),3.1(4)	0.2
					$\frac{5}{2}$		0.02(3)	0.4

[a] $\frac{5}{2}^+$ is rejected on the basis of the 6% branch to the 0.491 MeV $\frac{1}{2}^-$ level.

[b] Rejected by the branch to the 2.266 MeV $J=\frac{3}{2}$ level.

[c] Secondary transitions from the 1.988 MeV level are anisotropic.

[d] The parities of the $\frac{9}{2}$ levels are most likely even, on the grounds given by Ref. 20.

[e] $\frac{7}{2}^+$ is rejected by the branch to the ground state ($\frac{3}{2}^-$).

IV. DISCUSSION

A. Proton resonances

Most of the earlier studies of the ^{58}Ni(p,γ)^{59}Cu reaction concentrated on a small energy range or on a few isolated resonances. The only previous extensive yield curve was measured using the product positron activity.[19] In the region of overlap, up to 4 MeV, the agreement of the excitation function of Figs. 1 and 2 with that work is good. There are some significant differences between the present yield curve (Fig. 2) and the work of Klapdor *et al.*[25] For example, these authors report a single low spin resonance at 3.483 MeV, whereas we have found a high-spin—low-spin doublet 3.480-3.487 MeV. The $\frac{9}{2}^+$ nature of the 3.480 MeV resonance was suggested by Arai *et al.*[16] on the basis of its strong decay to the 3.042 MeV $\frac{9}{2}^+$ level. Earlier measurements of capture gamma ray angular distributions[25,26] resulted in spin assignments for seven resonances. An extensive set of two-angle (anisotropy) measurements by Hossain[33] is only partially supported by the present work.

The comparison with the results of elastic scattering is more difficult, though again the assignment of resonant energies agrees well, given the poorer resolution in the present experiment. The assignment of spins shows less agreement, except in the case of stronger (p,p) resonances. It is not surprising that the elastic scattering measure-

TABLE VI. Bound state spin-parity assignments.[a]

E_x (MeV)	Resonance No.	J^π This work	J^π Reference 1	Others	Reference
0			$\frac{3}{2}^-$		
0.491			$\frac{1}{2}^-$		
0.941			$\frac{5}{2}^-$		
1.399			$\frac{7}{2}^-$		
1.865	69	$\frac{7}{2}^-$	$\frac{7}{2}$		
1.988	43,49	$\frac{5}{2}^+$	$\frac{5}{2}$		
2.266			$\frac{3}{2}^+$		
2.318	65	$\frac{1}{2},\frac{5}{2}^-$	$\frac{1}{2}$	$\frac{1}{2}^-,\frac{3}{2}^-$	2,6,25
2.324	45	$\frac{3}{2}^-$	$\frac{3}{2}$		
2.587	49,102,108	$\frac{11}{2}^-$		$\geq\frac{7}{2}$	4,25
2.664	69	$\frac{5}{2}$-$\frac{11}{2}$	$\frac{5}{2},\frac{9}{2}$		
2.709	64,69	$\frac{5}{2}^-$	$\frac{5}{2}$	$\frac{5}{2}^-,\frac{7}{2}^-$	6,10
2.716	69,108	$\frac{7}{2}^-$	$\frac{7}{2}$		
2.928	69	$\frac{5}{2}^-$	$\frac{5}{2}$		
2.993	64,110	$\frac{3}{2},\frac{5}{2}^-,\frac{7}{2}^-$			
3.024	65	$\frac{5}{2}^-$	$\frac{5}{2},\frac{7}{2}$		
3.042			$\frac{9}{2}^+$		
3.115	35,69	$\frac{5}{2}^-$	$\frac{5}{2}$		
3.130	65	$\frac{1}{2}^-,\frac{3}{2},\frac{5}{2}^-$	$\frac{3}{2}^-$		
3.309	69	$\frac{7}{2}^-$		$\frac{7}{2}^+,\frac{9}{2}^+$	6
3.434	69	$\frac{5}{2}$	$\frac{5}{2}$		
3.438	64,92	$\frac{1}{2},\frac{3}{2},\frac{5}{2}$	$\frac{1}{2}$		
3.551	107	$\frac{5}{2}$	$\frac{5}{2}^-,\frac{7}{2}^-$		
3.574	64,69	$\frac{5}{2},\frac{7}{2}$			
3.578			$\frac{5}{2}^+$		
3.615	65	$\frac{3}{2}^-,\frac{5}{2}^-$	$\frac{3}{2}^-$		
3.699	64,69	$\frac{7}{2}$		$\frac{5}{2}^-,\frac{7}{2}^-$	6
3.729	110	$\frac{3}{2}^-,\frac{5}{2}$		$\frac{3}{2}^+,\frac{5}{2}^+$	5
3.742	95	$\frac{3}{2},\frac{5}{2}^+,\frac{7}{2}$	$\frac{3}{2}^-$		
3.756	108	$\frac{5}{2}^+,\frac{7}{2},\frac{9}{2}^-$	$\frac{1}{2}^-,\frac{3}{2}^-$	$\geq\frac{7}{2}$	25
3.887	69,95	$\frac{3}{2},\frac{5}{2}^+$	$\frac{3}{2}^-$		
3.906	65,69	$\frac{3}{2},\frac{5}{2},\frac{7}{2}^-$	$\frac{3}{2}^-$		
3.930	69	$\frac{5}{2},\frac{7}{2}$			
4.072	69	$\frac{3}{2},\frac{5}{2},\frac{7}{2}$		$\frac{7}{2}^+,\frac{9}{2}^+$	7
4.183	69	$\frac{5}{2},\frac{7}{2},\frac{9}{2}^-$	$\frac{5}{2},\frac{9}{2}$		
4.207	69	$\frac{5}{2},\frac{7}{2}^-$		$\frac{7}{2}^+,\frac{9}{2}^+$	7
4.301	64,69	$\frac{5}{2},\frac{7}{2}$		$\frac{5}{2}^-$	6,7,8,25
4.307	69	$\frac{5}{2}$		$\frac{5}{2}^-,\frac{7}{2}^-$	7
4.441	108	$\frac{7}{2}$		$\frac{7}{2}^+,\frac{9}{2}^+$	7
4.465	108	$\frac{5}{2}^+,\frac{7}{2},\frac{9}{2}^-$			
4.530	102,108	$\frac{5}{2}^+,\frac{7}{2},\frac{9}{2}^-$		$\frac{7}{2}^+,\frac{9}{2}^+$	7
4.917	108	$\frac{5}{2}^+,\frac{7}{2},\frac{9}{2}^-$		$\frac{7}{2}^+,\frac{9}{2}^+$	7

[a]Above 3.42 MeV the levels are proton unbound.

ments should miss a number of $l=3$ resonances, since their decay to the ^{58}Ni ground state is strongly suppressed by the angular momentum barrier. Such states therefore may easily be masked by lower spin resonances whose capture and inelastic cross sections may be much smaller.

The excitation function for inelastic scattering [Figs. 2(a) and 3] resembles closely that of Schiffer *et al.*,[14] with somewhat improved resolution. The spin determinations in the higher energy region, derived in the present work from the capture channel, agree reasonably with the earlier measurements from the angular distribution of the $2^+ \rightarrow 0^+$ γ transition in ^{58}Ni. The analysis of such angular distributions is particularly difficult when resonances may overlap, except in the case of $\frac{5}{2}^+$ resonances.

The present results are also in good agreement both in energy and angular momentum with the (^{3}He,d) experiments to unbound states,[7] especially below 7 MeV excitation in ^{59}Cu. Above this energy, the correlation between the capture and transfer reactions is less clear. For example, Ref. 7 names 16 $l=4$ transitions leading to $\frac{9}{2}^+$ levels. Of these, five are supported by d-p angular correlations. Our results, and those of Ref. 35, support the $\frac{9}{2}^+$ assignment for the strongest three of these, at 6.201, 6.847, and 6.916 MeV (energies of Ref. 7) and disagree with one at 6.310 MeV. The fifth, at 5.950 MeV, was not observed. Five lower-lying "$l=4$" levels were seen as resonances of final states in the present work, but none are $\frac{9}{2}^+$. Most would allow a $\frac{7}{2}^+$ assignment, among other possibilities. It is difficult to identify the resonances corresponding to the four remaining $l=4$ transitions because of the high level density.

B. Bound states

The systematic study of the γ decay of many resonances leads to a comprehensive view of the bound states of ^{59}Cu. Most of the 42 levels reported here were populated at several resonances (see Table IV), though their spins and parities depend on only one or two resonances from which they were strongly excited. The bound state properties in Tables IV and VI may be compared under three broad categories with previous work, summarized in Ref. 1. In the first and largest category are states clearly corresponding to those seen in previous high resolution gamma ray experiments and for which the spin-parity assignments are confirmed or revised. These include the above-mentioned five levels in Sec. III C: 1.865, 1.988, 2.324, 2.709, and 2.716 MeV. In all cases the spins are confirmed. The negative parities of the 1.865 and 2.716 MeV levels follow from their decays to the $\frac{3}{2}^-$ ground state and that of the 2.709 MeV level from its decay to the $\frac{1}{2}^-$ 0.491 MeV state. The 2.324 MeV state is fed by a strongly mixed transition from a $\frac{3}{2}^-$ resonance, No. 45. Similarly, the positive parity of the 1.988 MeV state is inferred from the large quadrupole content of the decay to it from a $\frac{3}{2}^+$ resonance, No. 43, and from its feeding from a $\frac{9}{2}^+$ resonance, No. 49. It is somewhat surprising to find two positive parity states (1.988 and 2.266 MeV) so low in energy in an upper fp-shell nucleus. Three further levels at 2.928, 3.024, and 3.115 MeV are all assigned $J^\pi = \frac{5}{2}^-$. The spin was determined from angular distributions and the parity inferred from the decays to the 0.491 MeV $\frac{1}{2}^-$ level. The 2.587 MeV level is fed only from the $\frac{9}{2}^+$ resonances and has spin $\frac{11}{2}$. Its negative parity follows from its decay to the 1.399 MeV $\frac{7}{2}^-$ state. For 12 other levels, at 2.318, 2.664, 3.130, 3.434, 3.438, 3.615, 3.742, 3.756, 3.887, 3.906, 4.183, and 4.301 MeV, the present results confirm the work of others. Of these states, the most notable are those at 3.887 and 3.906 MeV, reputed to be the split analog of the ^{59}Ni ground state.

The second category contains nine levels found in the present work and not previously reported in gamma ray studies. They may, however, correspond to levels seen in particle transfer reactions. These are the 3.309, 3.551, 3.699, 4.072, 4.207, 4.307, 4.441, 4.530, and 4.917 MeV states. The 3.729 MeV level spin assignment of $\frac{3}{2}$ or $\frac{5}{2}$ agrees with the $l=2$ finding from (^{3}He,d). The 3.551, 3.699, and 4.307 MeV levels correspond to $l=3$ proton stripping peaks and have compatible spins. The remaining six levels correspond to proton transfers assigned as $l=4$. In no case is $\frac{9}{2}^+$ among the possibilities allowed by the present angular distribution results. The 3.309 and 4.207 MeV levels could both have spin $\frac{7}{2}$, but both decay to the $\frac{3}{2}^-$ ground state making positive parity implausible. The 4.072, 4.441, 4.530, and 4.917 MeV levels allow, but do not demand, a $\frac{7}{2}^+$ interpretation.

Five levels found in this experiment have not previously been reported in either gamma ray or particle experiments. They are at 2.993, 3.574, 3.729, 3.930, and 4.465 MeV. The first is well established, having been observed at five resonances. Its spin is not unambiguously determined however. The 3.729 MeV state has $J=\frac{3}{2}$ or $\frac{5}{2}$, and the secondary decay to the 1.399 $\frac{7}{2}^-$ state requires negative parity if the spin is $\frac{3}{2}$. The 3.574 and 3.930 MeV levels are both limited to spins $\frac{5}{2}$ or $\frac{7}{2}$. The 4.465 MeV level was seen only in the decay of the main $\frac{9}{2}^+$ IAS but no angular distribution could be measured. The spin is limited by the formation and subsequent decay.

Several states reported in other gamma ray studies were not observed in this experiment. The 2.271 and 3.542 MeV levels reported by Klapdor *et al.*[25] in the decay of resonance 107 are likely the levels seen in this experiment at 2.266 and 3.551 MeV, although it is difficult to reconcile the energy differences since in general there is good agreement. Other levels reported by these authors, at 2.392, 3.084, 3.457, 3.785, 3.862, 4.131, and 4.689 MeV, were fed by weak branches from resonances 107 or 108. They were not found in the present work. Similarly, 2.459 and 3.663 MeV levels reported by Din and Al-Naser[24] and Trentelman *et al.*[26] at resonances 10 and 6, respectively, were not found in the present work. Two levels reported by Trentelman *et al.* at 3.022 and 3.025 MeV at resonances 26 and 22, respectively, were found to be a single level at 3.024 MeV in this work. A level at 4.053 MeV reported by Trentelman *et al.* at resonance 22 was not seen in the present study.

Among the many bound levels of ^{59}Cu there are several close doublets. Those at 2.318-2.324, 2.709-2.716, and 3.434-3.438 MeV were all previously reported by Trentelman *et al.*[26] They are confirmed by the present work, al-

TABLE VII. $T=\frac{3}{2}$ analog states for $A=59$.

^{59}Ni [a]			Resonance	^{59}Cu			
E_x (MeV)	J^π	$(2J+1)C^2S$	No.	E_x (MeV)	J^{π} [c]	$(2J+1)C^2S$	ΔE_C (MeV) [e]
0	$\frac{3}{2}^-$	2.6		3.887	$\frac{3}{2}^-$	0.61	9.469
				3.906	$\frac{3}{2}^-$	0.40	9.488
0.339	$\frac{5}{2}^-$	4.4		4.301	$\frac{5}{2}^-$		9.544
				4.307	$\frac{5}{2}^-,\frac{7}{2}^-$	2.14	9.550
0.465	$\frac{1}{2}^-$	1.2	1	4.347	$\frac{1}{2}^-$	0.48	9.464
0.878	$\frac{3}{2}^-$	0.29	6	4.769	$(\frac{3}{2},\frac{5}{2})$	0.05	9.473
			7	4.814	$\frac{3}{2}$	0.17	9.518
1.189	$\frac{5}{2}^-$		8	5.051	$(\frac{5}{2})^-$	0.14	9.444
1.302	$\frac{1}{2}^-$	0.54	10	5.227	$\frac{1}{2}^-,\frac{3}{2}^-$	0.21	9.507
1.338	$\frac{7}{2}^-$						
1.680	$\frac{5}{2}^-$	0.66	17	5.521	$\frac{3}{2}^-,\frac{5}{2}$	0.03	9.423
			19	5.550	$(\frac{3}{2},\frac{5}{2})$		9.452
1.735	$\frac{3}{2}^-$	0.03	22	5.602	$(\frac{3}{2})$	0.08	9.449
			23	5.608	$(\frac{3}{2})$ [d]		9.455
			25	5.642	$(\frac{3}{2},\frac{5}{2})$		9.489
1.739	$(\frac{9}{2}^-)$						
1.746							
1.767	$\frac{9}{2}^-$						
1.948	$\frac{7}{2}^-$	0.34	35	5.897	$\frac{7}{2}$	0.39	9.531
2.330	$\frac{5}{2}^-,\frac{7}{2}^-$						
			47	6.197	$(\frac{3}{2},\frac{5}{2})$		9.364
2.415	$\frac{3}{2}^-$	0.03	48	6.201	$(\frac{3}{2},\frac{5}{2})$		9.368
			50	6.238	$(\frac{3}{2},\frac{5}{2})$	0.03	9.495
2.634	$\frac{7}{2}^-$ [b]	0.31	69	6.493	$\frac{7}{2}$	0.42	9.441
2.681	$\frac{5}{2}^-$						
2.705	$\frac{11}{2}^-$						

TABLE VII. (*Continued*).

^{59}Ni [a] E_x (MeV)	J^{π}	$(2J+1)C^2S$	Resonance No.	^{59}Cu E_x (MeV)	$J^{\pi c}$	$(2J+1)C^2S$	ΔE_C (MeV) [e]
2.894	$\frac{3}{2}^-$	0.01	92	6.710	$\frac{3}{2}^-$		9.399
			93	6.727	$(\frac{3}{2},\frac{5}{2})$		9.416
3.026							
3.040	$\frac{7}{2}^{-\,b}$	0.12					
3.055	$\frac{9}{2}^+$	7.8	102	6.836	$\frac{9}{2}^+$	1.00	9.363
			108	6.905	$\frac{9}{2}^+$	1.70	9.432
3.127	$\frac{5}{2}^-,\frac{7}{2}^-$						
			110	6.939	$\frac{3}{2}^-$		9.340
3.182	$\frac{3}{2}^-$	0.03	111	6.945	$(\frac{3}{2})$	0.12	9.346
			113	6.967	$(\frac{3}{2},\frac{5}{2})$		9.368
3.460	$\frac{3}{2}^-$	0.14	131	7.332			9.454
			132	7.348	$\frac{3}{2}^-$		9.470
3.542	$(\frac{5}{2})^+$	0.18	134	7.394	$\frac{5}{2}$	0.23	9.434
3.578	$\frac{1}{2}^-,\frac{3}{2}^-$	0.09	137	7.444	$(\frac{3}{2})$		9.448
3.730	$\frac{5}{2}^-,\frac{7}{2}^-$		141	7.517	$(\frac{5}{2})$		9.369
3.865	$\frac{3}{2}^-$	0.10					
4.035	$\frac{1}{2}^-,\frac{3}{2}^-$	0.05					
4.155	$\frac{1}{2}^-,\frac{3}{2}^-$	0.07	169	8.013	$(\frac{3}{2})$		9.440

[a]Reference 1, with exceptions noted.
[b]Reference 36.
[c]This work and Refs. 2—11.
[d]Reference 33.
[e]For discussion of the uncertainties, see Sec. IV C.

though in a number of cases the decay branching is somewhat different from that previously given. The 3.578 MeV level is now joined by a companion at 3.574 MeV. The doublet 3.887-3.901 MeV was found by Din and Al-Naser[24] and was seen also in (^{3}He,d).[7,8] It is the lowest $T=\frac{3}{2}$ level. Another new doublet, and the second split analog state, is at 4.301-4.307 MeV.

C. Analog states

The identification of analog states among the many proton resonances in ^{59}Cu depends on two expected characteristics. There should be a roughly constant Coulomb energy difference ΔE_C between the analogs and their parent states, given by the difference in excitation energies and in ground state binding:

$$\Delta E_C = E_x(\text{Cu}) - E_x(\text{Ni}) + Q(\text{Cu}\rightarrow\text{Ni}) + Q(\text{n}\rightarrow\text{H}) .$$

Small variations of ΔE_C may be expected with excitation energy and with J^{π}, resulting from changes in the radial wave function from one state to another. Along with systematic energy comparisons, one expects proportionality between the spectroscopic factors for neutron and proton stripping to parent and analog states, respectively. At low energy, the level density is low enough to allow identification of proton resonances with peaks seen, for example, in the (^{3}He,d) reaction, and the above-mentioned criteria may be combined with confidence. At higher excitation energies, however, this is not possible, so the identification of isobaric analogs becomes more speculative. An additional difficulty is the lack of spin-parity information for many of the parent states at high excitation.

Table VII presents a list of proposed analog states. No uncertainties are given with the ΔE_C values, whose absolute errors are about 5—7 keV. This contains a systematic error of about 1.5 keV from the beta decay Q values.[1] The remainder arises from uncertainties in E_x in Ni and Cu, which are 1 keV or less for $E_x < 2$ MeV, ranging up to about 5 keV at $E_x = 3$ MeV for the states of interest. Within multiplets, however, much of this error is systematic, so the spreading widths suggested are probably reliable to 2 or 3 keV. Up to the 1.3 MeV ^{59}Ni state, the suggested analogs are the same as those proposed by others.[5,7,15] Above this, for the above-mentioned reasons, the assignments are less certain, though an attempt has been made to identify probable correspondences between

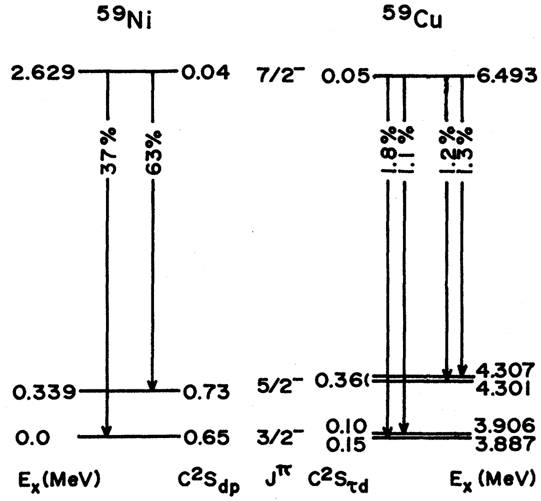

FIG. 8. Comparison of properties of three states of ^{59}Ni and their ^{59}Cu analogs. The analog of the 2.629 MeV ^{59}Ni level is the 6.493 MeV ^{59}Cu level excited at resonance 69. The decay from the resonance populates the lower analog doublets.

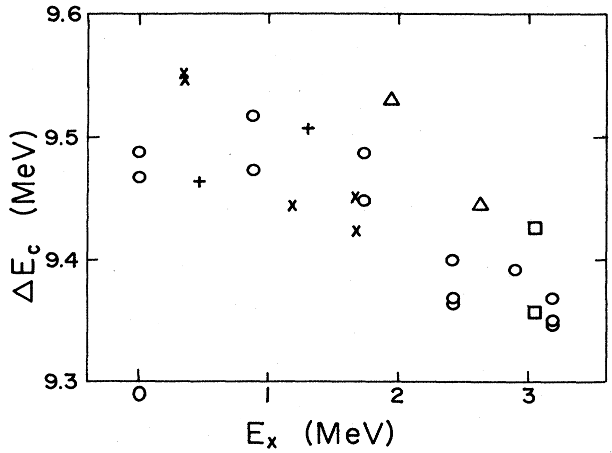

FIG. 9. Coulomb displacement energies for $T=\frac{3}{2}$ states in $A=59$. + denotes $\frac{1}{2}$, ○ denotes $\frac{3}{2}$, × denotes $\frac{5}{2}$, △ denotes $\frac{7}{2}$, and □ denotes $\frac{9}{2}$. The relative uncertainties are 1–2 keV, with a systematic error of 5–7 keV (see the text).

(^{3}He,d) and (p,γ) levels.

Consideration of the gamma decay of proposed analog states should be instructive. One would expect the decay branching of $T=\frac{3}{2}$ levels in ^{59}Cu to other $T=\frac{3}{2}$ levels to follow the same pattern as that in ^{59}Ni. Among the resonances studied, the only one which shows appreciable decay to lower $T=\frac{3}{2}$ levels is No. 69 (at $E_p=3.131$, $E_x=6.493$ MeV). The analogy to the supposed parent, at 2.629 MeV in ^{59}Ni, is illustrated in Fig. 8. It will be observed that while the ratio of spectroscopic factors between the ^{59}Ni ground state and its split analog is 2.7, compared to 3.0, the ratio of squares of isospin Clebsch-Gordan coefficients, this is not the case for the higher states. The gamma branching ratios are also only in qualitative agreement. On the other hand, the branching of the 6.493 MeV ^{59}Cu level to the two fragments of the ground state analog is proportional to the ratio of their spectroscopic factors, as expected.

Figure 9 illustrates the general trend of the Coulomb displacement energies to decrease as expected with increasing excitation energy. No clear angular momentum dependence is discernable. The variations to be expected may be estimated in the following way. The Coulomb displacement energy depends on

$$\langle \psi_p \mid V_C \mid \psi_p \rangle - \langle \psi_n \mid V_C \mid \psi_n \rangle ,$$

where V_C is the Coulomb potential of the ^{58}Ni core and ψ_p and ψ_n are the wave functions of the odd proton and neutron analog states in ^{59}Cu and ^{59}Ni, respectively. The second term vanishes. Since V_C decreases with increasing radius, one would expect states of higher excitation energy or higher angular momentum to have lower displacement energies. The first half of this naive expectation is confirmed by calculation using single-particle wave functions in a Woods-Saxon potential. The second is not. Indeed, the reverse is true—calculated displacement energies for higher l values are greater than those for lower l. This effect may be attributed to the centrifugal barrier which suppresses the exterior part of the wave function to which the Coulomb energy is particularly sensitive. At higher excitation energy at least, the experimental displacement energies for higher l values, 3 and 4, seem slightly larger than those for lower spin states at similar energies.

In spite of the rapid rise of the level density with E_x, little increase of the spreading width of analog state multiplets is seen. If this is confirmed by more detailed studies of individual multiplets, it would suggest, as proposed in Ref. 45, that the effects of external mixing with nearby states of lower isospin is less important than those caused by simple low energy excitations, weakly coupled to the analog states. The contribution to the spreading of analog state strength from the mixing of parent states is probably significant at the higher excitation energies.

V. CONCLUSIONS

In the present high resolution investigation, the decay properties of a large number of proton resonances in ^{59}Cu have been found. Many of the resonances are candidates as analogs of ^{59}Ni states. A considerable addition has been made to available information about bound states of ^{59}Cu, through the establishment of four new levels and eight others previously unobserved at high resolution. For a number of the levels, spin and parity and decay schemes have been revised.

ACKNOWLEDGMENTS

The authors acknowledge the hospitality and assistance of scientists at all the laboratories where the experiments reported here were performed. In particular, thanks are due to J. R. Leslie and W. McLatchie (Queen's), V. Meyer (Zürich), A. Gallmann (Strasbourg), H. Fuchs (Hahn-Meitner Institute), and A. Antilla (Helsinki). This work was supported in part by grants from the Natural Sciences and Engineering Research Council of Canada.

[1]P. Andersson, L. P. Ekström, and J. Lyttkens, Nucl. Data. Sheets **39**, 641 (1983).
[2]J. Bommer, H. Fuchs, K. Grabisch, H. Kluge, W. Ribbe, and G. Röschert, Nucl. Phys. **A199**, 115 (1973).
[3]D. J. Pullen and B. Rosner, Phys. Rev. **170**, 1034 (1968).
[4]R. O. Nelson, C. R. Gould, D. R. Tilley, and N. R. Roberson, Phys. Rev. C **9**, 2193 (1974).
[5]P. K. Bindal, D. H. Youngblood, and R. L. Kozub, Phys. Rev. C **14**, 521 (1976).
[6]R. M. Britton and D. L. Watson, Nucl. Phys. **A272**, 91 (1976).
[7]S. Galès, S. Fortier, H. Laurent, J. M. Maison, and J. P. Schapira, Nucl. Phys. **A268**, 257 (1976); **A280**, 499 (1977).
[8]J. P. Schapira, J. M. Maison, M. N. Rao, S. Fortier, S. Galès, and H. Laurent, Phys. Rev. C **17**, 1588 (1978).
[9]N. Matsuoka *et al.*, Nucl. Phys. **A373**, 377 (1982).
[10]P. Roussel, G. Bruge, A. Buissière, H. Faraggi, and J. E. Testoni, Nucl. Phys. **A155**, 306 (1970).
[11]P. Viatte, S. Micek, R. Müller, J. Lang, J. Unternährer, C. M. Teodorescu, and L. Jarczyk, Helv. Phys. Acta **49**, 569 (1976).
[12]J. Honkanen, M. Kortelahti, K. Eskola, and K. Vierinen, Nucl. Phys. **A366**, 109 (1981).
[13]Y. Arai, M. Fujioka, E. Tanaka, T. Shinozuka, H. Miyatoka, M. Yoshii, and T. Ishimatsu, Phys. Lett. **104B**, 186 (1981).
[14]J. P. Schiffer, M. S. Moore, and C. M. Class, Phys. Rev. **104**, 1661 (1956).
[15]J. C. Browne, H. W. Newson, E. G. Bilpuch, and G. E. Mitchell, Nucl. Phys. **A153**, 481 (1970).
[16]E. Arai, M. Ogawa, and H. Sato, Nucl. Phys. **A256**, 127 (1976).
[17]A. E. Antropov, N. P. Zarubin, and I. D. Ioannu, Izv. Akad. Nauk SSSR Ser. Fiz. **41**, No. 10, 2210 (1977).
[18]J. W. Butler and C. R. Gossett, Phys. Rev. **108**, 1473 (1957).
[19]J. H. Carver and G. A. Jones, Nucl. Phys. **19**, 184 (1960).
[20]S. Maripuu, Phys. Lett. **31B**, 181 (1970).
[21]I. Fodor, I. Szentpétery, and J. Szücs, Phys. Lett. **32B**, 689 (1970).
[22]S. Maripuu, J. C. Manthuruthil, and C. P. Poirier, Phys. Lett. **41B**, 148 (1972).
[23]I. Szentpetery and J. Szücs, Phys. Rev. Lett. **28**, 378 (1972).
[24]G. U. Din and A. M. Al-Naser, Aust. J. Phys. **28**, 503 (1975).
[25]H. V. Klapdor, M. Schrader, G. Bergdolt, and A. M. Bergdolt, Nucl. Phys. **A245**, 133 (1975).
[26]J. P. Trentelman, B. E. Cooke, J. R. Leslie, W. McLatchie, and B. C. Robertson, Nucl. Phys. **A246**, 457 (1975).
[27]B. E. Cooke, J. R. Leslie, and B. C. Robertson, Can. J. Phys. **53**, 2506 (1975).
[28]B. E. Cooke, J. R. Leslie, W. McLatchie, and B. C. Robertson, J. Phys. G **3**, 391 (1977).
[29]O. E. Kraft, Yu. V. Naumov, S. S. Parzhitskii, B. F. Petrov, Z. Salekh, and I. V. Sizov, Izv. Akad. Nauk. SSSR, Ser. Fiz. **41**, No. 1, 82 (1977).
[30]M. D. Hossain, Nuovo Cimento **39A**, 594 (1977).
[31]O. E. Kraft, Yu. V. Naumov, S. S. Parzhitskii, B. F. Petrov, V. M. Sigalov, and I. V. Sizov, Izv. Akad. Nauk. SSSR, Ser. Fiz. **43**, No. 5, 1083 (1979).
[32]B. E. Cooke, J. R. Leslie, W. McLatchie, and P. Skensved, Can. J. Phys. **58**, 359 (1980).
[33]M. D. Hossain, Nuovo Cimento **60A**, 157 (1980).
[34]G. U. Din and J. A. Cameron, Eastern Regional Nuclear Physics Conference 1978 (unpublished).
[35]I. M. Szöghy and C. Rangacharyulu, Can. J. Phys. **60**, 959 (1982).
[36]G. A. Huttlin, J. A. Aymar, J. A. Bieszk, S. Sen, and A. A. Rollefson, Nucl. Phys. **A263**, 445 (1976).
[37]M. Pichevar, J. Delaunay, B. Delaunay, H. J. Kim, Y. El Masri, and J. Vervier, Nucl. Phys. **A264**, 445 (1976).
[38]P. Sen, C. Sen, and D. Basu, Z. Phys. A **280**, 211 (1977).
[39]A. F. M. Ishaq, A. Robertson, W. V. Prestwich, and T. J. Kennett, Z. Phys. A **281**, 365 (1977).
[40]P. Staub, E. Baumgartner, J. X. Saladin, H. Schär, and D. Trautmann, Helv. Phys. Acta. **50**, 9 (1977).
[41]H. Ikegami, T. Yamazaki, S. Morinobu, I. Katayama, M. Fujiwara, Y. Fujita, and N. Koori, Phys. Lett. **74B**, 326 (1978).
[42]W. R. Zimmerman, J. J. Kraushaar, M. J. Schneider, and H. Rudolph, Nucl. Phys. **A297**, 263 (1978).
[43]E. R. Flynn, R. E. Brown, F. D. Correll, D. L. Hanson, and R. A. Hardekopf, Phys. Rev. Lett. **42**, 626 (1979).
[44]T. Taylor and J. A. Cameron, Nucl. Phys. **A337**, 389 (1980).
[45]E. G. Bilpuch, A. M. Lane, G. E. Mitchell, and J. D. Moses, Phys. Lett. **28C**, 145 (1976).
[46]J. A. Cameron, Can. J. Phys **62**, 115 (1984).
[47]S. Cohen, R. D. Lawson, M. H. Macfarlane, S. P. Pandya, and M. Soga, Phys. Rev. **160**, 903 (1967).
[48]N. Auerbach, Phys. Rev. **163**, 1203 (1967).
[49]P. W. M. Glaudemans, M. J. A. de Voigt, and E. F. M. Steffens, Nucl. Phys. **A198**, 609 (1972).
[50]R. P. Singh, R. Raj, M. L. Rustgi, and H. W. Kung, Phys. Rev. C **2**, 1715 (1970).
[51]J. E. Koops and P. W. M. Glaudemans, Z. Phys. A **280**, 181 (1977).
[52]B. Castel, I. P. Johnstone, B. P. Singh, and K. W. C. Steward, Can. J. Phys. **50**, 1630 (1972).
[53]R. E. Azuma, L. E. Carlson, A. M. Charlesworth, K. P. Jackson, N. Anyas-Weiss, and B. Lalović, Can. J. Phys. **44**, 3075 (1966).
[54]A. J. Ferguson, *Angular Correlation Methods in Gamma-Ray Spectroscopy* (North-Holland, Amsterdam, 1965).
[55]H. J. Rose and D. M. Brink, Rev. Mod. Phys. **39**, 306 (1967).